Mechanical properties and microstructure characterization of Eurofer97 steel variants in EUROfusion program

Xiang Chen[a], Arunodaya Bhattacharya[a], Mikhail A. Sokolov[a], Logan N. Clowers[a], Yukinori Yamamoto[a], Tim Graening[b], Kory D. Linton[a], Yutai Katoh[a], Michael Rieth[b]

[a]Oak Ridge National Laboratory, Oak Ridge, Tennessee, USA
[b]Karlsruhe Institute of Technology, Karlsruhe, Baden-Württemberg, Germany

Eurofer97 steel is the European reference structural material for the first wall and blanket of DEMO fusion reactor. The harsh environment of a fusion reactor, such as neutron irradiation and He damage, results in significant degradation of the mechanical properties, e.g. fracture toughness. Characterization of fracture toughness for fusion structural materials is necessary to ensure long-term safe operation of the fusion reactor. To achieve this goal, we have developed a fracture toughness testing technique using pre-cracked miniature multi-notch bend bar specimens based on the Master Curve method. Under the framework of EUROfusion, we characterized the pre-irradiation fracture toughness of ten Eurofer97 variants along with their Vickers hardness and tensile properties. We then elucidate the composition/heat treatment-microstructure-property relationships for select materials.

Keywords: mechanical properties, fracture toughness, Master Curve, small specimen testing technique, Eurofer97.

1. Introduction

Eurofer97 steel is the European reference structural material for the first wall and blanket of a DEMO fusion reactor [[1]-[3]]. For neutron irradiation temperatures < ~350-370 °C, Eurofer97 steel is known to suffer from irradiation induced ductile-brittle transition temperature (DBTT) shift with resulting fracture toughness degradation. Therefore, characterization of fracture toughness is necessary to ensure long-term safe operation of the fusion reactor. For neutron-irradiated specimens which are usually much smaller than standard size specimens due to limited volume of irradiation facilities and advantages with testing small size specimens, such as lower radioactivity and more accurate control of irradiation temperatures, there is a need to develop fracture toughness testing procedure that is representative of bulk specimens. To achieve this goal, we have developed a fracture toughness testing technique using pre-cracked miniature multi-notch bend bar (referred as M4CVN hereafter) specimens based on the Master Curve method. Under the framework of EUROfusion, we characterized the pre-irradiation fracture toughness, combined with Vickers hardness, tensile, and microstructure of ten Eurofer97 steel variants that were fabricated using non-standard routes. Further, same materials were irradiated at the High Flux Isotope Reactor (HFIR) of Oak Ridge National Laboratory (ORNL) at ~300°C to 2.5 dpa (displacement per atom) and will be tested in future to study the neutron irradiation effect.

2. Experimental

2.1 Materials

Ten Eurofer97 variants (E, H, I, J, K, L, M, N, O, and P) were provided for testing. The material compositions are listed in Table 1 with heat treatment/processing conditions in Table 2. The compositions of E and M are same as a standard Eurofer97 and the heat treatment condition of E represents the standard heat treatment for Eurofer97.

Table 1. Compositions of ten Eurofer97 variants (wt%)

Mat.	Cr	C	Mn	V	N	W	Ta	Si
P	8.7	.11	.02	.20	.045	1.1	.09	.03
H	8.7	.06	.02	.35	.047	1.1	.10	.04
I	8.7	.11	.02	.35	.042	1.1	.09	.04
E,M	8.8	.11	.53	.20	.019	1.1	.12	.04
L	9.1	.11	.54	.20	.038	1.1	.12	.03
J	9.0	.11	.39	.22	.022	1.1	.11	<.04
K	7.8	.02	<.03	.22	.022	1.0	.13	<.04
O	8.8	.06	.50	.30	.070	1.0	.05	.15
N	9.0	.09	.11	<.05	.002	1.0	.09	.04

Table 2. Heat treatment conditions of ten Eurofer97 variants

Mat.	Heat treatment conditions[*]
P	1000°C/0.5h+WQ+820°C+AC
H	1000°C/0.5h+WQ+820°C+AC
I	1000°C/0.5h+WQ+820°C+AC
E[**]	980°C/0.5h+AQ+760°C+AC
M	1020°C/0.5h+AQ+1020°C/0.5h+AQ+760°C/1.5h+AC
L	1150°C/0.5h+AQ+700°C+AC
J	1250°C/1h+rolling to a final rolling temperature of 850°C in 6 rolling steps with a reduction of 20-30% for each step+AC+ 880°C/0.5h+WQ+750°C/2h+AC
K	1250°C/1h+rolling to a final rolling temperature of 850°C in 6 rolling steps with a reduction of 20-30% for each step+AC+1050°C/0.25h+WQ+675°C/1.5h+AC
O	1080°C/1h, cooling to 650°C and rolling to 40% reduction+760°C/1h+AC
N	920°C/1.5h+AQ+920°C/1.5h+AQ+760°C/1h+AC

[*]AQ: air quench; WQ: water quench; AC: air cooled
[**]E had experienced an unknown heat treatment prior to the shown heat treatment.

2.2 Methods

We conducted Vickers hardness testing based on the ASTM E384 standard [4] using 1kgf load and 15 s dwell time. We performed at least ten measurements on each variant, on SS-J3 grip sections, to obtain an average hardness value.

Tensile testing was conducted at room temperature on SS-J3 type miniature tensile specimens (gauge dimension: 5 x 1.2 x 0.75 mm^3) based on the ASTM E8 standard [5]. The specimen loading direction follows the rolling direction of the raw material. The applied strain rate was 10^{-3} s^{-1} with machine stroke control. We tested at least two tensile specimens for each variant.

Fracture toughness testing was performed using M4CVN specimens according to the Master Curve method in the ASTM E1921 standard [6]. At least 14 notches were tested per variant. The M4CVN specimen (dimension: 45x3.3x1.65 mm^3) was developed in the US Fusion material program and has four notches per specimen . The specimen follows the same size ratio of the bend bar specimen in ASTM E1921. Since the loading portions between neighboring notches are shared, the M4CVN specimen consumes much less material than the standard single notch bend bar specimen and is favorable for neutron irradiation testing. To test such small specimens, we have designed a dedicated testing fixture shown in Fig. 1. The deflection gauge measures the load-line displacement of the specimen. The push bar slides left /right and is used to push the specimen against the positioning block to ensure specimen notch aligns with the indenter and the deflection gauge. All specimens were machined in L-T orientation except for E from which specimens were machined in the L-S orientation. Each notch was fatigue pre-cracked to a crack size to width ratio of 0.44-0.5. During testing, liquid nitrogen was used to control the testing temperatures which were measured directly from thermocouple wires welded to the specimens. Detailed experimental setup and testing procedures can be found in [7].
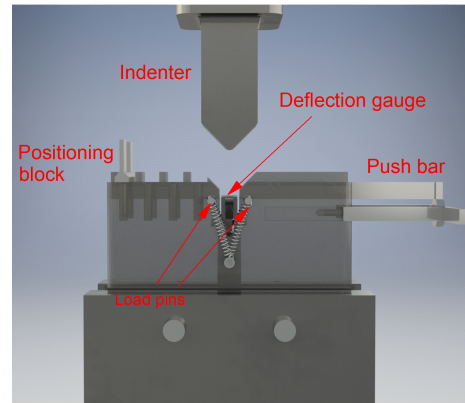

Fig. 1 M4CVN specimen test fixture.

Lastly, we performed microstructure characterization using optical microscopy (OM), scanning electron microscopy (SEM), and scanning-transmission electron microscopy (STEM) with energy-dispersive X-ray spectroscopy (EDS). For OM and SEM, the samples were polished to mirror polish and etched in Villella's reagent. STEM was performed on focused ion beam (FIB) lift out specimens using a XFEG based 200kV FEI F200X Talos STEM, while Hitachi S4800 FEG-SEM was used for SEM. FIB samples were prepared using FEI Quanta DualBeam FIB, with 30 kV for initial liftout and 2kV for final polishing step. OM and SEM were performed on the rolling direction-normal direction (RD-ND) plane from undeformed head/grip sections of the tensile specimens. Readers are referred to [8] for more details on microstructure characterization technique.

3. Results and discussion

3.1 Vickers hardness and tensile properties

Vickers hardness and tensile results for the ten Eurofer97 variants are shown in Fig. 2 and Fig. 3, respectively. The reference Eurofer97 hardness [9] and tensile strength values [10] are overlaid as dashed lines in the same figures for comparison. Most steel variants showed similar hardness as the reference Eurofer97 except for H with slightly lower hardness and K and L with significantly higher hardness. The yield and ultimate tensile strengths showed in general a similar trend as the hardness results, i.e. lower strength for H and much high strengths for K and L. However, except

for M and O, other steel variants (I, J, N, P, and E) with similar hardness values as the reference Eurofer97 exhibited lower strengths than the reference material.
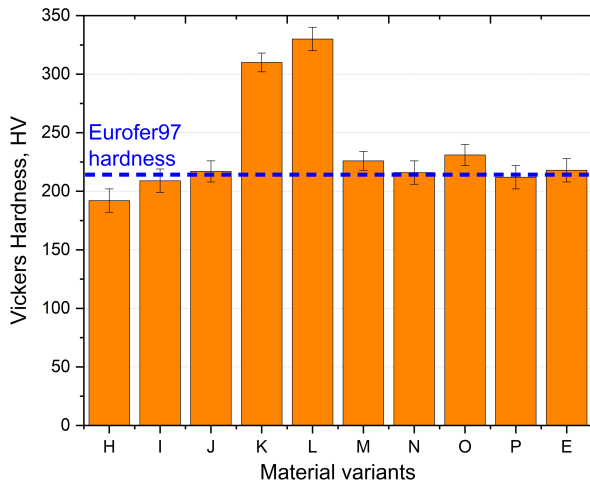

Fig. 2 Vickers hardness of ten Eurofer97 variants in comparison with reference Eurofer97.
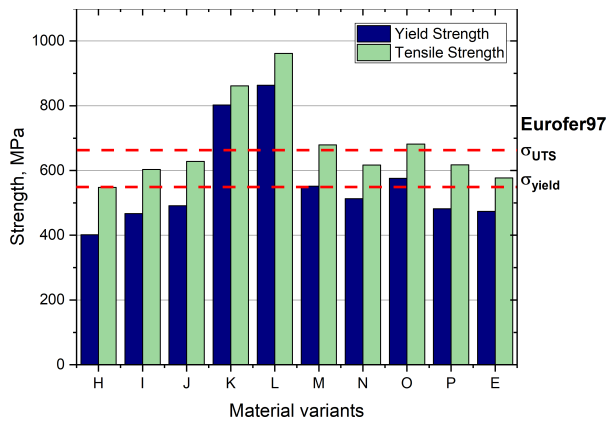

Fig. 3 Yield and ultimate tensile strengths of ten Eurofer97 variants in comparison with reference Eurofer97.

3.2 Fracture toughness transition temperatures

In Fig. 4, we compare the Master Curve transition temperature T_0 results for the ten Eurofer97 variants with the T_0 range of reference Eurofer97 from literature [7]. Most steel variants are within the upper scatter band of the reference material range. However, E, K, and L showed much higher T_0 than the reference Eurfer97, indicating worse fracture toughness.
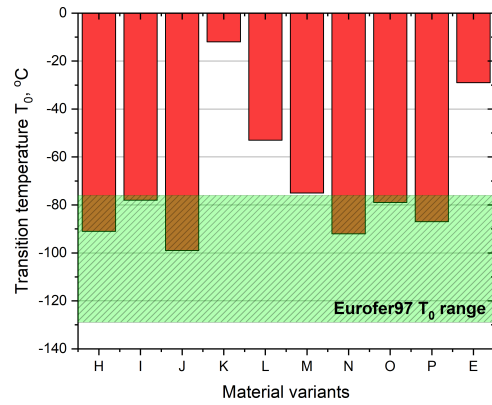

Fig. 4 Transition temperature T_0 of ten Eurofer97 variants in comparison with the T_0 range of reference Eurofer97.

3.3 Microstructure

Selected microstructure results are presented here to elucidate the composition/heat treatment-microstructure-property relationships for four Eurofer97 variants, specifically the ones which had the worse fracture toughness (K,L,E) and a double-austenized steel (M). Complete microstructure results can be found in [8].

OM and STEM-EDX images for K are shown in Fig. 5. K exhibited coarser grain structure than reference Eurofer97. The large grain size is unfavorable for fracture toughness of Eurofer97 [11] and likely resulted from the high normalization temperature (1050°C). The low tempering temperature (675°C) may not have fully tempered the martensite structure, resulting in higher hardness and strength but poorer fracture toughness. Therefore, we attribute the low fracture toughness to a combination of large grain size and undertempering. In addition, K has very low carbon content (0.02wt%), which is needed to stabilize austenite and the transformed martensite. The low carbon content, and low tempering temperature also resulted in very few precipitates found in this material (Fig. 6b), which may cause lower creep strength and accelerated grain growth of the material at high temperatures. Lastly, lack of manganese in K (<0.03wt%) can also be of concern since manganese is an essential element for increasing the hardenability, acting as deoxidant in hot rolling, and combining with sulfur to counters the brittleness of the steel.
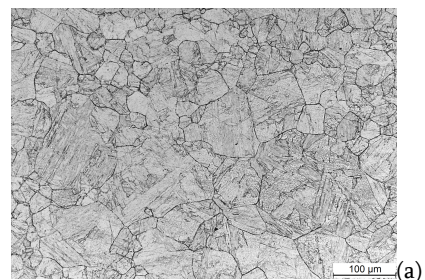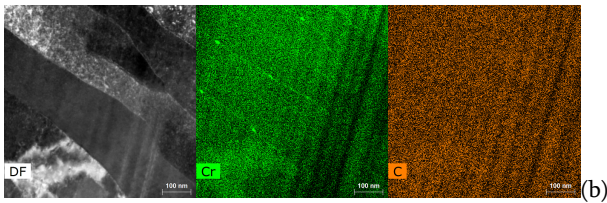
Fig. 5 K optical image in (a) and low-angle annular dark-field (DF) STEM with EDS maps in (b)

OM and STEM images with EDS maps for L are shown in Fig. 6. The combination of high normalization (1150°C) and low tempering (700°C) temperatures for this material also resulted in a coarse under-tempered martensite microstructure, which is again linked with higher hardness and strength but poorer fracture toughness. Also, high nitrogen (380 ppm) in this material may additionally result in the increased hardness /strength, and reduced toughness. But C content and tempering temperature was higher than in K which formed precipitates in L that were mainly Cr, W rich (expected $M_{23}C_6$ carbides) and Cr, V rich expected to be M_2X nitrides [12]. No evidence of pure Ta, V rich MX was noted.
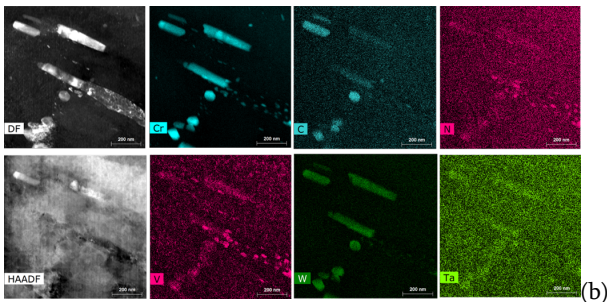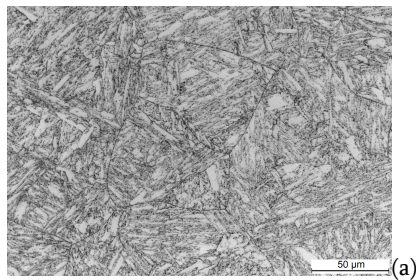

Fig. 6 L optical image in (a) and (DF), high-angle annular dark field (HAADF) STEM images with EDS maps in (b)

OM, SEM, and STEM-EDS images for E are shown in Fig. 7. The material exhibited a heterogeneous microstructure with a non-uniform distribution of coarse precipitates (>1 μm), which are larger than typical precipitates expected for a standard Eurofer97 (Fig. 8b). These coarse precipitates were best revealed in optical/SEM images than in STEM that focuses on a very small area. STEM-EDS maps showed the precipitates in E were typical Cr, W rich consistent with $M_{23}C_6$ carbides and Ta, V rich consistent with MX carbonitrides, normally observed in standard Eurofer97. Although the prior-austenite grain

boundaries and lath boundaries for a tempered martensite microstructure was visible in E, the prior-austenite grain size also seemed larger than a reference Eurofer97, and a homogeneous distribution of fine precipitates on these boundaries and inside grains were absent. These microstructure features most likely resulted in the lower strength and toughness for this material. Due to the unknown prior heat treatment conditions for E, it is difficult to determine the exact factors resulting in the final microstructure.
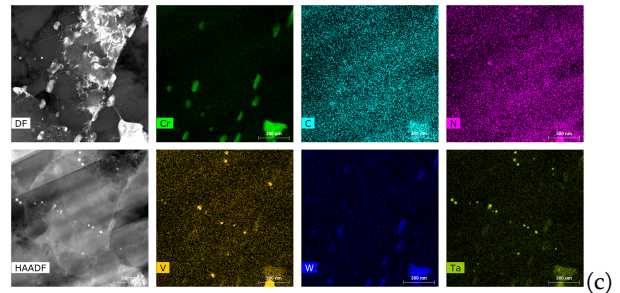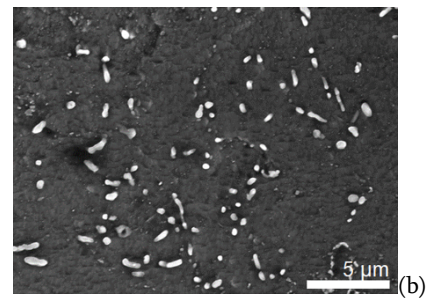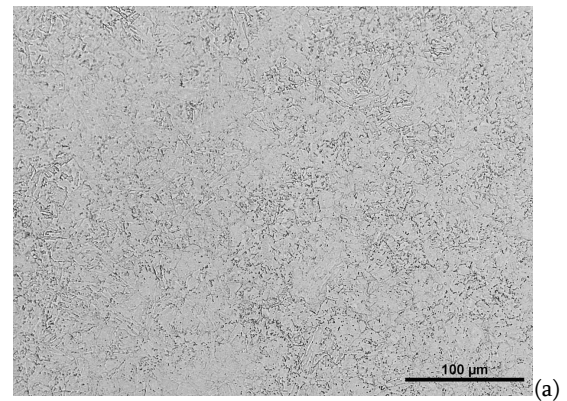

Fig. 7 E OM image in (a), SEM secondary electron image in (b) and DF, HAADF and STEM-EDS maps in (c)

OM and STEM - EDS maps for M are shown in Fig. 8. M had the same composition as a reference Eurofer97,but went through a double austenitization cycle. The material exhibited typical refined tempered martensite microstructure with Cr, W rich $M_{23}C_6$ carbides and Ta, V rich MX carbonitrides. Mechanical properties were in line with reference Eurofer97, indicating no obvious beneficial effect of double austenitization on the mechanical properties for this material.
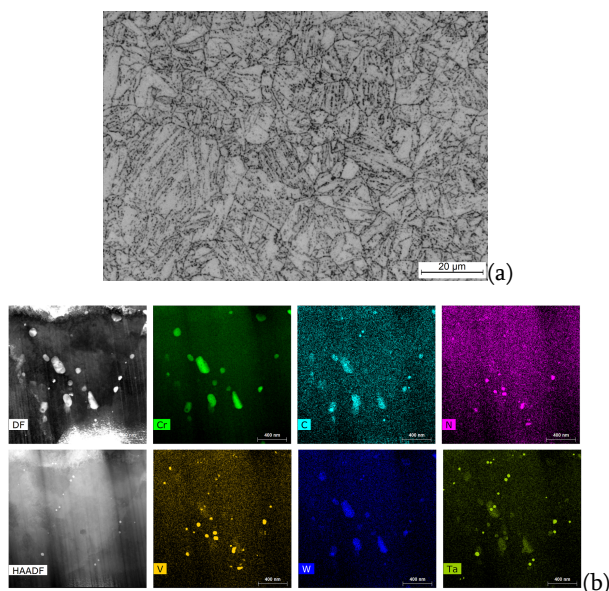
Fig. 8 M OM image in (a) and DF, HAADF and STEM-EDS maps in (b)

4. Conclusions

We characterized the pre-irradiation transition fracture toughness of ten Eurofer97 variants along with their Vickers hardness, tensile properties, and microstructure. Compared with a reference Eurfoer97, the ten variants didn't show a comprehensive improvement of mechanical properties. In addition, the composition and microstructures adverse to fracture toughness , such as low Mn and C contents, coarse grain size, under-tempered martensite, lack of precipitation, and coarse non-uniform distribution of precipitates, have been identified in some steel variants. Further studies will be performed on same materials after neutron irradiation.

Acknowledgments

References

[1] A. Kohyama et al., Low-activation ferritic and martentistic steels for fusion application, Journal of Nuclear Materials 233-237 (1996) 138-147.

[2] P. Fernández et al., Metallurgical characterization of the reduced activation ferritic/martensitic steel Eurofer'97 on as-received condition, Fusion Engineering and Design 58-59 (2001) 787-792.

[3] N. Baluc et al., Status of reduced activation ferritic/martensitic steel development, Journal of Nuclear Materials 367-370 (2007) 33-41.

[4] ASTM E384-17, Standard Test Method for Microindentation Hardness of Materials, ASTM International, West Conshohocken, PA, 2017

[5] ASTM E8 / E8M-16a, Standard Test Methods for Tension Testing of Metallic Materials, ASTM International, West Conshohocken, PA, 2016.

[6] ASTM E1921-17a, Standard Test Method for Determination of Reference Temperature, To, for Ferritic Steels in the Transition Range, ASTM International, West Conshohocken, PA, 2017.

[7] X. Chen et al., Master Curve fracture toughness characterization of Eurofer97 using miniature multi-notch bend bar specimens for fusion applications, Proceedings of the ASME 2018 Pressure Vessels and Piping Conference, PVP2018-85065, July 15-20, 2018, Prague, Czech Republic.

[8] Bhattacharya et al., Mechanical properties and microstructure characterization of unirradiated Eurofer-97 steel variants for the EUROfusion project, ORNL/SPR-2018/882, doi:10.2172/1471901.

[9] N. Ilchuk et al., Fracture toughness characterization in the lower transition of neutron irradiated Eurofer97 steel, Journal of Nuclear Materials 442 (2013) S58-S61.

[10] C. Petersen, Post irradiation examination of RAF/M steels after fast reactor irradiation up to 33 dpa and < 340°C (ARBOR1) RAFM steels metallurgical and mechanical characterization, FZKA 7517, 2010.

[11] M. Rieth et al., EUROFER 97 Tensile, Charpy, creep and structural tests, FZKA 6911, 2003.

[12] Henry et al., Improvement of Eurofer 97 high-temperature mechanical properties using non-standard heat treatments, 17th International Conference on Fusion Reactor Materials, October 11-16, 2015, Aachen, Germany